An Analysis of Gradient-Induced Distortion in Dual Beam ATI Systems for Vector Surface Current Mapping

Mark A. Sletten
Naval Research Laboratory, Code 7264
4555 Overlook Ave. SW
Washington DC 20375
mark.sletten@nrl.navy.mil

***Abstract*— This paper summarizes an analysis of gradient-induced distortions in the vector surface current estimates generated by dual-beam, along-track interferometric SAR systems. In such systems, interferograms from two squinted beams, one squinted forward of broadside and the other aft, are combined to measure the full surface current vector with only a single aircraft pass. However, in the presence of significant current gradients, an effect akin to velocity-bunching can cause distortion in the measured current estimates. Up to a point, these distortions can be removed by a straightforward, spatial re-mapping of the interferogram pixels based upon their phase values. However, there is a critical current gradient beyond which the true surface current field is not recoverable. In addition, the along-track component of the surface current introduces unequal azimuthal displacements in the fore- and aft-squinted interferograms. As a result, when along-track currents are present, the two interferograms will not be spatially registered. If appreciable along-track current gradients are also present, the resulting current vector estimates in and around the gradient region will undergo further distortion. These effects are explored through an approximate, linear analysis as well as through a full interferometric SAR model, using the current gradients present in rivers as an example.**

Keywords-SAR interferometry; currents

I. INTRODUCTION

The idea of using a dual-beam, along-track interferometer (ATI) to measure the ocean surface current vector with only a single aircraft pass was first suggested by *Rodriguez* et al [1]. *Frasier and Camps* [2] developed this concept in more detail and presented an analysis of a proposed system, the Dual Beam Interferometer (DBI), which has since been constructed and recently demonstrated in the field [3, 4]. However, in the presence of significant current gradients, an effect akin to velocity-bunching can cause distortion in the measured current estimates. For some viewing geometries, the amount of distortion will be different in the two beams, thus compounding the problem. This paper presents the results of an investigation to determine if and when this distortion mechanism is significant and under what conditions the resulting error can be corrected.

II. DESCRIPTION OF DISTORTION MECHANISM

With a dual-beam ATI, data from two independent interferometers, one squinted forward of broadside by an angle θ_s, the other squinted aft by the same amount, are combined to generate estimates of the along- and cross-track components of the surface velocity, $\hat{v}_x$ and $\hat{v}_y$:

$$\hat{v}_x(x) = \frac{u_r^+(x) - u_r^-(x)}{2\sin\theta_s \sin\theta_i} \qquad \hat{v}_y(x) = \frac{u_r^+(x) + u_r^-(x)}{2\cos\theta_s \sin\theta_i} \quad . \quad (1)$$

$u_r^+(x)$ and $u_r^-(x)$ are the radial velocities measured by the fore- and aft-squinted ATI beams, and θ_i is the incidence angle. x is the coordinate in the along-track, or azimuthal, direction, while the range coordinate is suppressed as it plays no role in this analysis. These equations are applied pixel-by-pixel to the pair of fore and aft interferograms to produce a surface velocity map. However, an issue that has not been fully addressed is related to the fact that the mapping from a given point on the true surface to the corresponding point in an interferogram involves an azimuthal displacement that is proportional to the radial current at that point. Specifically, if the current *varies* in the along-track direction, neither the fore- nor the aft-squinted beam will capture an accurate representation of the gradient of the radial current viewed by that beam, since the azimuthal displacement will vary across the gradient region in proportion to the varying current. The current profile in both beams will thus be stretched or compressed relative to the true profile, not merely offset. This effect is closely related to velocity bunching, an important SAR imaging mechanism for ocean waves, and is the primary distortion mechanism discussed in this paper. Note that this distortion can occur in a single-beam, non-squinted system as well as in a dual-beam, vector ATI.

While the amount of distortion at a given point will depend on the details of the actual current profile in which it is embedded, a localized, linear analysis can still be used to investigate this distortion effect in a general way. Neglecting spatial resolution effects for the moment and assuming the current gradient always has a value below a critical limit (defined below), the following expressions relate the true radial

This work was performed at the Naval Research Laboratory under the "Physics of INSAR-Based Ocean Surface Current Measurement" program, Work Unit 8027.

US Government work not protected by US Copyright

Report Documentation Page

Form Approved
OMB No. 0704-0188

Public reporting burden for the collection of information is estimated to average 1 hour per response, including the time for reviewing instructions, searching existing data sources, gathering and maintaining the data needed, and completing and reviewing the collection of information. Send comments regarding this burden estimate or any other aspect of this collection of information, including suggestions for reducing this burden, to Washington Headquarters Services, Directorate for Information Operations and Reports, 1215 Jefferson Davis Highway, Suite 1204, Arlington VA 22202-4302. Respondents should be aware that notwithstanding any other provision of law, no person shall be subject to a penalty for failing to comply with a collection of information if it does not display a currently valid OMB control number.

1. REPORT DATE	2. REPORT TYPE	3. DATES COVERED
25 JUL 2005	**N/A**	**-**

4. TITLE AND SUBTITLE	5a. CONTRACT NUMBER
An Analysis of Gradient-Induced Distortion in Dual Beam ATI Systems for Vector Surface Current Mapping	5b. GRANT NUMBER
	5c. PROGRAM ELEMENT NUMBER
6. AUTHOR(S)	5d. PROJECT NUMBER
	5e. TASK NUMBER
	5f. WORK UNIT NUMBER
7. PERFORMING ORGANIZATION NAME(S) AND ADDRESS(ES) **Naval Research Laboratory, Code 7264 4555 Overlook Ave. SW Washington DC 20375**	8. PERFORMING ORGANIZATION REPORT NUMBER
9. SPONSORING/MONITORING AGENCY NAME(S) AND ADDRESS(ES)	10. SPONSOR/MONITOR'S ACRONYM(S)
	11. SPONSOR/MONITOR'S REPORT NUMBER(S)

12. DISTRIBUTION/AVAILABILITY STATEMENT
Approved for public release, distribution unlimited

13. SUPPLEMENTARY NOTES
See also ADM001850, 2005 IEEE International Geoscience and Remote Sensing Symposium Proceedings (25th) (IGARSS 2005) Held in Seoul, Korea on 25-29 July 2005. , The original document contains color images.

14. ABSTRACT

15. SUBJECT TERMS

16. SECURITY CLASSIFICATION OF:			17. LIMITATION OF ABSTRACT	18. NUMBER OF PAGES	19a. NAME OF RESPONSIBLE PERSON
a. REPORT	b. ABSTRACT	c. THIS PAGE			
unclassified	**unclassified**	**unclassified**	**UU**	**4**	

current at an arbitrary along-track position, $u_r^{\pm}(x)$, to the radial current in the interferogram at the same point, $u_{ri}^{\pm}(x)$:

$$u_r^{\pm}(x) = u_{ri}^{\pm}(x + D_r^{\pm}(x)) \quad (2)$$

$$u_{ri}^{\pm}(x) = u_r^{\pm}(x - D_{ri}^{\pm}(x)) \quad (3)$$

where

$$D_r^{\pm} = -\frac{R}{v_p} u_r^{\pm} \quad (4)$$

$$D_{ri}^{\pm}(x) = -\frac{R}{v_p} u_{ri}^{\pm}(x) \quad (5)$$

are the azimuthal displacements as a function of position computed using the true radial velocity and the shifted interferogram velocity, respectively. R is the distance (range) from the platform to the point on the surface, v_p is the platform velocity, and "+" and "–" refer to the fore and aft beams. Equation (2) describes the forward problem in which a given current element on the water surface is mapped into points in the fore and aft interferograms. Equation (3) describes the inverse problem, in which the two interferograms can be mapped back to the true surface.

Assuming the radial velocity gradients vary relatively slowly in the azimuth direction, (3) can be approximated and combined with (5) to produce the following expression for the approximate interferogram radial velocities in terms of the values and gradients of the true velocity field:

$$\hat{u}_{ri}^{\pm} = \frac{u_r^{\pm}}{1 - \frac{R}{v_p}\frac{du_r^{\pm}}{dx}} \quad (6)$$

Note that at the critical gradient values $du_r^{\pm}/dx = v_p/R$, the solution given by (6) diverges. At this value of the gradient, the mapping from the true current field to the interferograms becomes multi-valued, and the phase of the interferogram pixel is no longer simply related to the current at a single point on the surface. Fig. 1 is a schematic representation of this potentially multi-valued mapping for three (below critical, critical, and above critical) assumed values of v_p/R. In this illustration, the current is assumed to be flowing away from the radar while increasing, from left to right, from a value of zero. The aircraft is assumed to be flying from left to right with the radar looking off the port side (i.e. off the left side, when looking in the direction of flight). The relationship between the gradient direction and the flight direction determine whether the gradient will be compressed or stretched in the interferogram. Assuming the conventions that a positive current is one that flows away from the aircraft and that the aircraft flies in the positive *x*-direction, compression will occur when the current gradient is positive, and stretching will occur when the gradient is negative.

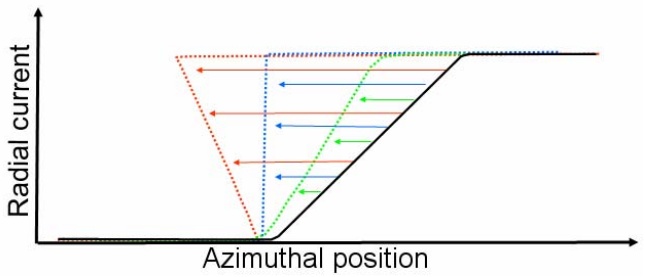

Fig. 1. Schematic illustration of the displacement of a current profile (black) assuming a gradient value below the critical value (green), at the critical value (blue) and above the critical value (red).

In a dual-beam, squinted ATI, both beams can suffer this gradient-induced distortion, but to differing degrees. In the presence of an *along-track* current component, the angles between the current and the fore and aft beams will not be equal, and thus the radial velocities measured by the two beams will be unequal as well. This creates mis-alignment between the fore and aft interferograms and additional errors in the estimated velocity vectors. This vector distortion can be better understood by solving (1) for the radial velocities,

$$u_r^{\pm} = \sin\theta_i \left(\pm v_x \sin\theta_s + v_y \cos\theta_s \right) \quad (7)$$

and then inspecting the expressions for the fore and aft azimuthal displacements in (4). It can be seen that in the presence of an along-track surface velocity v_x, the fore and aft currents, and thus the fore and aft displacements, will not be equal. In these regions, the interferograms will not be aligned. If an azimuthal gradient in the surface velocity is also present, the estimated velocity vector at this common point will be distorted. The *cross-track* component of the velocity, v_y, also introduces a displacement, but one that is common to both the fore and aft beams. It only introduces an azimuthal shift, but no magnitude or direction errors, in the velocity estimates.

With one caveat, the technique to correct these displacement errors is straightforward. Before combining the interferograms to compute the estimated along- and cross-track velocities, each pixel in the fore and aft interferograms should be shifted back by $D_{ri}^{\pm}$, according to (3). After this remapping process, the new interferograms can be interpolated and resampled on a regular grid, and the corrected velocities estimated. However, regions over which the gradient meets or exceeds the critical value v_p/R will not be imaged accurately, even after this correction, since the interferometric phase at any point in these regions will not be proportional to the current in any single resolution cell on the surface, but will instead be determined by a weighted combination of the current values at several distinct, and possibly widely separated, cells. Under such conditions, the details of the current profile cannot be recovered by remapping the pixels. The size of the region over which this unrecoverable distortion occurs is proportional to the difference between the actual and critical gradients as well as the transition region width. This effect is investigated using a full ATI model in the next section.

III. RIVER EXAMPLE

Strong currents (2 m/s or more) and strong current gradients occur often in rivers, and there is presently interest in using ATI to measure these flows remotely [5]. In this section, a full ATI model is used to investigate the limitations imposed by the gradient distortion mechanism when an ATI is used to measure spatial flow patterns in such an environment.

The ATI model used in this investigation is that developed by *Frasier and Camps* for analysis of the DBI [2]. The values of the important model parameters were assumed to be as follows: fore and aft squint angles, 20°; radar frequency, 5.3 GHz; altitude, 600 m; aircraft velocity, 100 m/s; surface coherence time, 50 ms; aperture integration time 150 ms; ratio of land to river radar cross section, 1000:1; incidence angle, 70°; fore-aft antenna spacing, 1.0 m. The selected surface coherence time is based upon recent river measurements by *Plant* [5]. The resulting spatial resolution is approximately 10 m.

The "canonical" river flow pattern used as an input to the model is displayed as red vectors in Figs 2, 3, and 4. It contains three gradient regions: one each near the left and right banks (located at ±150 m), and another between them that might represent, for instance, the edge of a high current region induced by a deep channel on the right side of the river. Between these regions are an area on the left with a constant current of 0.5 m/s and another on the right representing the high current in the channel

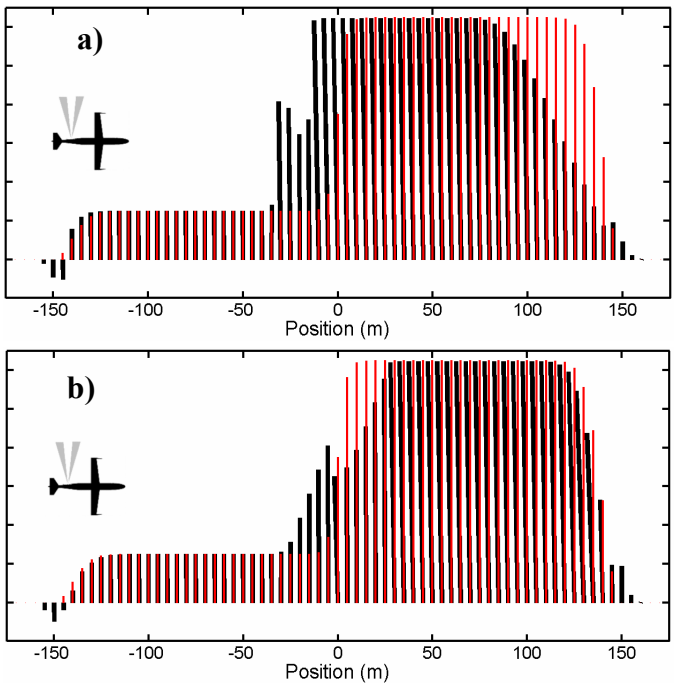

Fig. 2. Actual (red) and predicted (black) vector currents, assuming a perpendicular transect angle across the river. a) Predicted currents before correction for displacements. b) Predicted currents after correction.

with a constant current of 2.5 m/s. The gradients near the left and right banks are described by the function $(1-\sin^n(x\pi/w))$, where w is the river width and n is a large integer. (w=300 m and n=100 in this particular case.) The middle gradient near x=0 follows the form of a hyperbolic tangent, ~tanh(x/d), where in this case, the transition width, d, is 12.5 m. From left to right, the gradients of these three regions, normalized by the critical gradient $v_p/R = 0.057$, are approximately 0.4, 2.5 and -2.2.

Fig. 2 shows the currents predicted by the model assuming the aircraft is flying across the river in the positive x-direction, perpendicular to the direction of current flow, with the ATI looking off to the port (left) side. This viewing geometry is indicated by the aircraft silhouette. The black lines in Fig. 2a are the predicted current vectors before correcting the interferograms for the azimuthal displacements. The central transition is distorted and shifted to the left, while the gradient region near the right bank is stretched out significantly. Some magnitude distortion also occurs in the left bank gradient, but it is comparatively insignificant. Fig. 2b shows the predicted current vectors after correcting the interferogram displacements. The central transition is still significantly distorted, owing to the fact that the gradient is over twice the critical value. The right bank gradient, however, has been all but restored. Even though the gradient magnitude is high near the right bank, the direction of the gradient relative to the aircraft flight direction is such that the displaced current profile is stretched, not compressed and forced to fold over itself, and is therefore correctable.

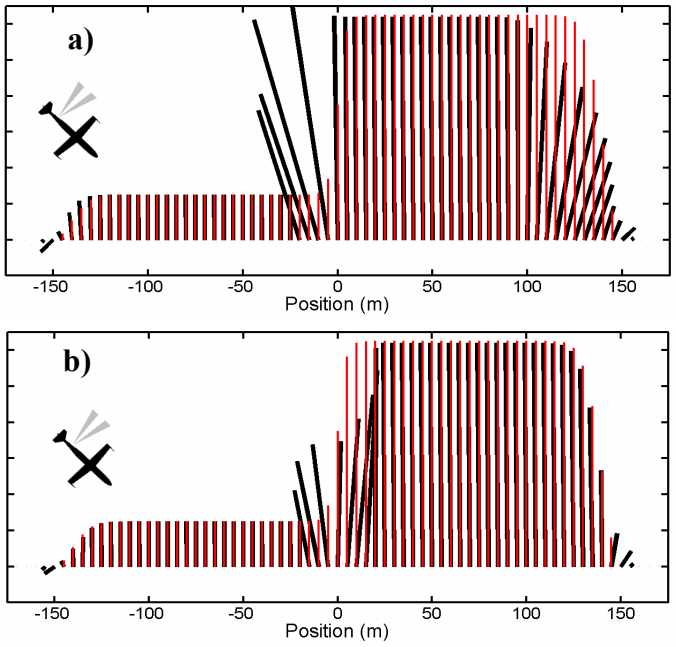

Fig. 3. Actual (red) and predicted (black) vector currents, assuming a 45° transect angle across the river. a) Predicted currents before correction for displacements. b) Predicted currents after correction.

Fig. 3 illustrates the effect of the aircraft flight direction on the distortion. As indicated by the silhouette, the aircraft is assumed to be flying at a 45° angle to the current flow in this figure. As seen in Fig. 3a, both magnitude as well as direction errors occur in the predicted vectors, and as shown in Fig. 3b, significant magnitude and direction errors remain even after correcting the interferograms. This additional distortion arises due to the fact that when the aircraft flies across the river at an

angle, a component of the river current lies in the along-track direction. As discussed in the previous section, this introduces misalignment between the fore and aft interferograms in the gradient region and thus additional distortion.

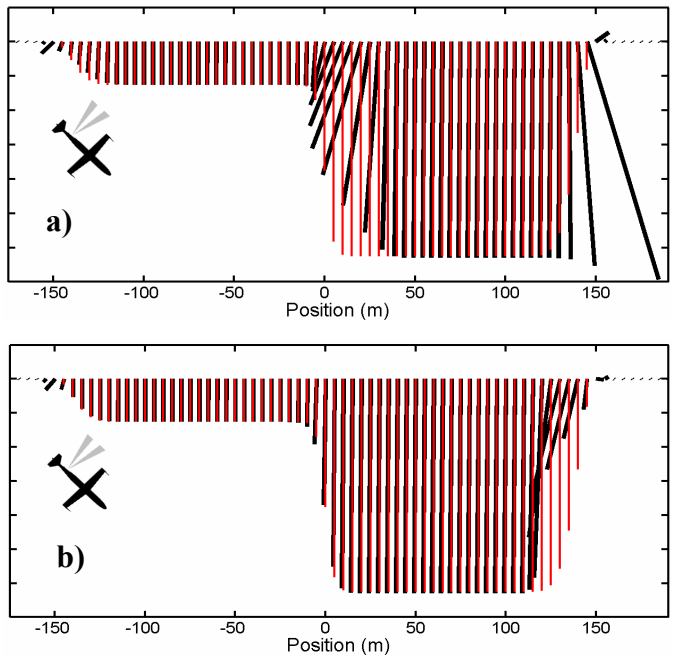

Fig. 4. Actual (red) and predicted (black) vector currents, assuming a 45° transect angle across the river and a reversed flow direction relative to Figs. 2 and 3. a) Predicted currents before correction for displacements. b) Predicted currents after correction.

Figure 4 emphasizes the importance of the flight direction relative to the current even further. In this figure, the direction of the current flow has been reversed while the aircraft transect angle has been kept at 45°. In this case, it is the gradient region near the right bank that suffers from uncorrectable distortion. The presence of the nearby land, which is of course stationary and which has a high radar cross section, affects the details of the distortion in this transition region. Over the land itself, contributions from displaced river signals are negligible, and thus the ATI velocity of the bank is (correctly) zero.

IV. Conclusion

This paper summarizes the results of an investigation of the distortion induced in ATI surface current estimates by current gradients. The primary mechanism is closely related to velocity-bunching, a mechanism responsible for SAR imaging of ocean waves. The results indicate that the distortion may be significant if an airborne ATI is used to estimate the strong current gradients found in rivers. The analysis and examples also show that if the gradient exceeds a critical value, distortion remains even after applying a correction technique in which the current-induced azimuthal displacements are accounted for.

References

[1] Rodriguez, E., D. Imel, and B. Houshmand, "Two-dimensional surface currents using vector along-track interferometry", in *Proceedings of PIERS '95*, Seattle, WA, p. 763, 1995.

[2] Frasier, S.J., and A. Camps, "Dual-beam interferometry for ocean surface current vector mapping", *IEEE Transactions on Geoscience and Remote Sensing*, vol. 39, no. 2, February, 2001.

[3] Farquharson, G. et al, "A pod-based dual beam SAR", *IEEE Geoscience and Remote Sensing Letters*, vol. 1, no. 2, April 2004.

[4] Toporkov, J.V., D. Perkovic, G. Farquharson, M.A. Sletten, and S.J. Frasier, "Sea surface velocity vector retrieval using dual-beam interferometry: first demonstration", *IEEE Transactions on Geoscience and Remote Sensing*, in press.

[5] Plant, W.J., W.C. Keller, and K. Hayes, "Measurement of river surface currents with coherent microwave systems", *IEEE Transactions on Geoscience and Remote Sensing*, in press.